RSC Advances

PAPER

View Article Online
View Journal | View Issue

Cite this: *RSC Adv.*, 2022, **12**, 27055

Preparation and controlled-release properties of a dual-response acidizing corrosion inhibitor

Yang Zhitao,[ab] Yang Yuhua,*[ab] Zhao Haojie[ab] and Miao Changrui[ab]

Received 22nd July 2022
Accepted 14th September 2022

DOI: 10.1039/d2ra04540k

rsc.li/rsc-advances

In this study, HMSNs with a specific surface area of 900 $m^2\ g^{-1}$ and a wall thickness of 50 nm were prepared by a soft template method. A cavity structure with a diameter of about 150 nm was constructed between the core and shell, and it had a mesoporous structure of 4.0 nm. Therefore, the core and shell particles have an ideal carrying capacity as a corrosion inhibitor carrier. Amino modified HMSNs and grafted ferrocene group to obtain FcHMSNs. Impregnation method and negative pressure method were used to load acidizing corrosion inhibitor, and nano-valves sensitive to REDOX potential and pH were used to block the mesopores of HMSNs. The acidizing inhibitor (DR-HMSNs@S-AFA) was completely encapsulated in micro/nano containers. The controlled release performance of DR-HMSNs@S-AFA acidizing inhibitor was studied. The results showed that the acidizing inhibitor with DR-HMSNs@S-AFA load could achieve rapid release under strong acidic conditions or a certain concentration of H_2O_2.

1. Introduction

There is increasing interest in developing stimulation responsive active substance delivery systems to improve the effect and prolong the action of active substances.[1–4] A large and relatively stable active substance repository is necessary for a high-quality delivery system. Compared with polymer nanoparticles, micelles and vesicles, nano-sized hollow mesoporous silica (HMSNs) with hollow interior (drug storage) and microporous shell (controlled release) have higher application value in drug slow/controlled release, with good biocompatibility. Its advantages such as low toxicity and side effects also make it widely used as a drug slow-release/controlled-release carrier, and it is a very promising drug delivery system.[5–8] However, HMSNs without any modification have very limited slow-release and controlled-release ability for active substances, so installing switches, sensitive to environmental factors, in the release channel has been considered. For the field of metal corrosion protection, researchers considered loading corrosion inhibitors into HMSNs nanocontainers, and using inorganic nanoparticles, organic molecules, biomolecules and other capping agents as gatekeepers to realize the controlled release of corrosion inhibitors, so as to respond to a series of stimuli, such as pH, redox, light, electromagnetic, *etc.*[9–11]

HMSNs nanocarrier systems assembled with nano valves are promising carriers for controlling drug delivery because they are able to move or change one component of the nano valves and release the active substance in the container in a specific target in response to external stimuli, such as chemical, photochemical or electrochemical pulses. Accurate selection of recognition sites is a very important step in the controlled release system. If the size, shape and properties of nano valve components cannot be perfectly matched, the whole encapsulated controlled release system may leak.[12,13] From this perspective, the subject β-cyclodextrin (β-CD) and guest ferrocenyl (–Fc) have been successfully used to construct rotaxanes, supramolecular dendrimers and recently mechanized nanoparticles. First described in 1975 β-inclusion of ferrocene by CD.[14–16] Recently, Stoddart's team prepared a nano valves by immobilizing ferrocene dicarboxylic acid on amino functionalized nanoparticles loaded with rhodamine B dye and using β-CD termination. The attempt to open the nano valves pores was carried out under alkaline conditions, which deprotonated the ferrocene carboxylate acid group, exulting in the repulsion between carboxylate anions and β-electrostatic and then the release of dyes.[17–20]

As an important additive for metal corrosion protection, corrosion inhibitor has the characteristics of high volatility and high price. In the process of oil well acidification, it is also easy to lose and lose efficacy, resulting in huge waste. In this paper, a simple, efficient and environmentally friendly nano container with stable performance, large capacity and high specific surface area was prepared for storage of corrosion inhibitors, and then designed and assembled on its surface β-CD inclusion ferrocene nano valves. The controlled release properties were measured in different pH and oxidation environments. This not only greatly improves the stability of the corrosion inhibitor, but also provides an experimental basis for the "on-demand release" of the corrosion inhibitor, and lays a good foundation for extending the service life of steel equipment in the oil well acidification system.

[a]*Lanzhou Jiaotong University, College of Chemistry and Chemical Engineering, China. E-mail: 934512581@qq.com*

[b]*Institute of Water Treatment Chemistry, China*

2. Materials and methods

The work described here aims to construct a nano container with high efficiency and rapid release of inhibitor under strong acidic conditions or high oxidant concentration, which was assembled with β-cyclodextrin coated ferrocene nanovalves. It is well known that ferrocene in the presence of strong acid is oxidized by molecular oxygen to corresponding quantitative radical ions by protonation. Therefore, the preparation of our nano capsule was carried out in the following process (1) HMSNs were surface modified with 3-aminopropyl tri methoxy silane (APTMS), (2) functionalized with ferrocene formaldehyde, (3) loaded with acidifying corrosion inhibitor, and (4) the pore was closed with β-CD (Fig. 1).

2.1. Materials

Acetophenone ($C_6H_5OCH_3$, AR, 99%), ethanolamine (C_2H_7NO, AR, 99%), formaldehyde (HCHO, AR, 37 ∼ 40%), concentrated hydrochloric acid (HCl, AR, 36 ∼ 38%), potassium iodide (KI, AR, 99%), *tert*-butyl acrylate (*t*-BA : $C_7H_{12}O_2$, AR, 99%), poly-(*t*-butyl acrylate) (PTBA), potassium persulfate (KPS, AR, 99%), ammonia ($NH_3 \cdot H_2O$, AR, 25 ∼ 28%), tetraethyl orthosilicate (TEOS, AR, 99%), cetyl trimethyl ammonium bromide (CTAB, AR, 99%), sodium carbonate (Na_2CO_3, AR, 99%), 3-aminopropyl trimethoxy silane (APTMS, AR, 99%), ferrocenecarboxaldehyde (FcCHO : $C_{11}H_{10}FeO$, AR, 98%), sodium borohydride ($NaBH_4$, AR, 98%), toluene ($C_6H_5CH_3$, AR, 99.9%), β-cyclodextrin (β-CD, BR, 99%), ammonium nitrate (NH_4NO_3, AR, 98%), corrosion inhibitor (S-AFA, Made in a laboratory, 99%).

2.2. Synthesis of template PTBA nanospheres

In this paper, PTBA nanospheres were prepared by conventional emulsion polymerization. The mixed solution of CTAB, 80 mL deionized water and 2 mL *tert*-butyl acrylate (*t*-BA) was stirred quickly for 30 min in nitrogen atmosphere at 60 °C, then 5 mL potassium persulfate (KPS) aqueous solution (0.10 M) was added, and 10 mL *t*-BA was added at a constant rate within 2 hours. After the addition, the reaction continued for 3 hours, resulting in a very homogeneous and stable white emulsion in water called PTBA emulsion, which, even after a week, showed almost no change compared with the previous state. As shown in Fig. 2.

2.3. Synthesis of PTBA@SiO_2-CTAB nanospheres

0.60 g PTBA emulsion was weighed and evenly dispersed with a mixture of 20 mL anhydrous ethanol and a certain amount of deionized water. Then 0.32 g CTAB was added to the above dispersion with 15 mL deionized water at constant volume. The mixed solution was stirred at a rate of 1000 rpm at 40 °C for 30 min. Finally, 1.0 mL ammonia solution (25 wt%) and 1.20 mL TEOS were successively added to the above mixture for 24 hours. After the reaction, the mixture was centrifuged, the supernatant was discarded, and the white powder at the bottom of the centrifugation tube was centrifuged and washed twice with deionized water and anhydrous ethanol, respectively, to obtain the SiO_2 shell containing micelle wrapped by PTBA nanospheres (PTBA@SiO_2-CTAB).

2.4. Synthesis of HMSNs

PTBA@SiO_2-CTAB was stirred in ethanol solution of NH_4NO_3 (10 mg·mL^{-1}) at a speed of 600 rpm at 85 °C for reflux for 1 h. After the reaction, the solution was centrifuged and the supernatant was discarded. The white powder at the bottom of the centrifuge tube was centrifuged and washed twice with deionized water, and then centrifuged and washed three times with anhydrous ethanol to obtain HMSNs, which was dried for 12 h in a constant temperature drying oven at 80 °C for later use. The

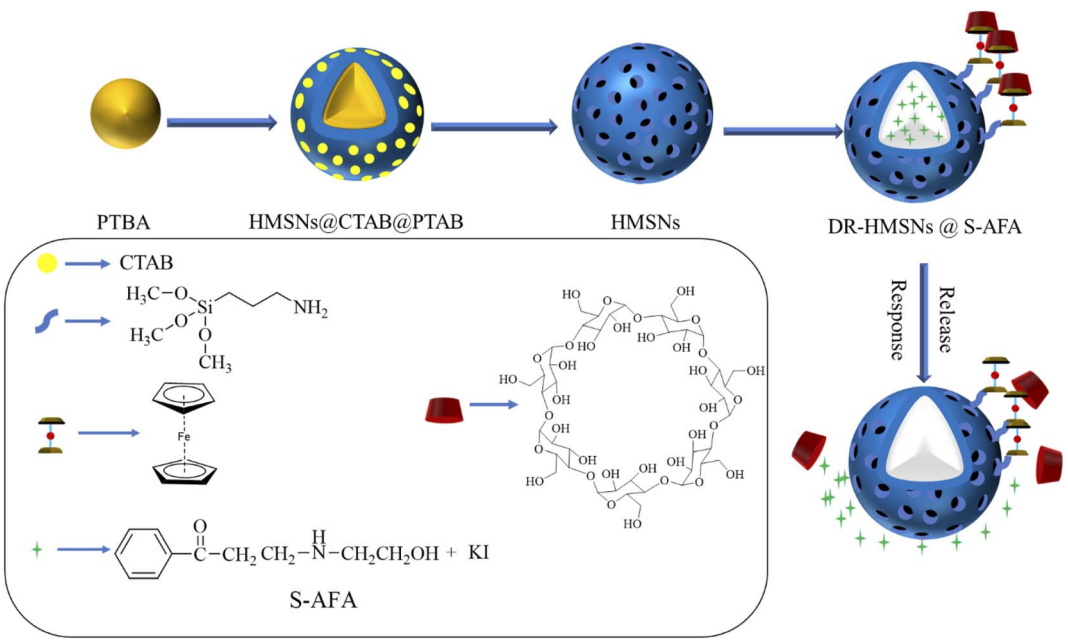

Fig. 1 Operation of ferrocenyl functionalized nano-reservoir group, load corrosion inhibitor, cover β-CD.

Fig. 2 PTBA emulsion.

process of preparing HMSNs by soft template method is shown as Fig. 3.

2.5. Modification of HMSNs

2.5.1 Amino modification. 0.25 g HMSNs was suspended in 30 mL dried toluene containing 2.5 mL 3-aminopropyl trimeth oxysilane (APTMS). The solution was stirred, condensed and reflow at 80 °C nitrogen atmosphere for 12 h, then the products were collected, centrifuged and precipitated with anhydrous ethanol, washed by ultrasonic for several times, and dried in a constant temperature drying oven at 40 °C for 24 h to obtain aminopropyl hollow mesoporous silica (APHMSNs).

2.5.2 Graft ferrocene formaldehyde. In a nitrogen atmosphere, 15 mL anhydrous ethanol solution containing 0.25 g ferrocene formaldehyde was placed in a 100 mL three-mouth flask and stirred for 1 h in a dark environment at room temperature. Then 0.25 g degassed solid APHMSNs was slowly added to obtain the suspension, which was stirred in a nitrogen atmosphere at room temperature for 1 h. The reaction mixture was cooled to room temperature, 0.028 g sodium borohydride was added, and then stirred for 1 h, the mixture was poured into the centrifuge tube at the speed of 2500 rpm, the supernatant was discarded, and then washed with deionized water and ethanol for several times. The mixture was dried in a constant temperature drying oven at 80 °C for 24 h to obtain orange solid. The grafted ferrocene-based hollow mesoporous silica (FcHMSNs).

2.6. Loading acidizing corrosion inhibitor

Load acidizing corrosion inhibitor using impregnation method and negative pressure method. To be specific, first put 0.25 g FcHMSNs into a 100 mL three-necked flask, connect a vacuum pump to vacuum, maintain the pressure at 0.075–0.08 MPa, and inject 3 mL acidification corrosion inhibitor with a syringe from one side of the flask. The vacuum pump was closed by vacuum-pumping the three-port flask with HMSNs, and the slow injection of corrosion inhibitor was stopped when the pressure in the vessel remained constant. These two operations were repeated alternately until FcHMSNs was just immersed by acidification corrosion inhibitor, and the FcHMSNs loaded with acidification corrosion inhibitor is recorded as FCHMSN@S-AFA. After loading, the nano valves was directly installed without taking out (Fig. 4).

The properties of acidifying corrosion inhibitor (S-AFA) was evaluated with reference to "SY/T 5405-2019 corrosion inhibitor performance test method and evaluation index for acidification", and the corrosion medium was 20% hydrochloric acid, the corrosion temperature was 60 °C, the corrosion time was 4 h, and the inhibitor dosage was 0.5 wt%.

2.7. Installation of FcHMSNs nano valves

200 mg β-cyclodextrin was added into a three-mouth flask containing FcHMSN@S-AFA and stirred at 600 rpm for 24 h. After the reaction, it was centrifuged into a centrifuge tube at a speed of 2500 rpm and centrifuged and washed with deionized water for several times to remove the unloaded acidification corrosion inhibitor and β-cyclodextrin, and dried at 60 °C for 24 h to obtain dual-response nanoparticles (DR-HMSNs@S-AFA) containing acidification corrosion inhibitor.

2.8. Study on controlled release performance

In this paper, a hollow mesoporous silica carrier modified by β-cyclodextrin inclusion ferrocene nano valves loaded with acidizing corrosion inhibitor was designed to study the response release of acidizing corrosion inhibitor. HMSNs was coated with β-cyclodextrin and ferrocene nano valves to form core–shell structure. The hollow and mesoporous structure of HMSNs is used as the storage unit of acidizing corrosion inhibitor, while

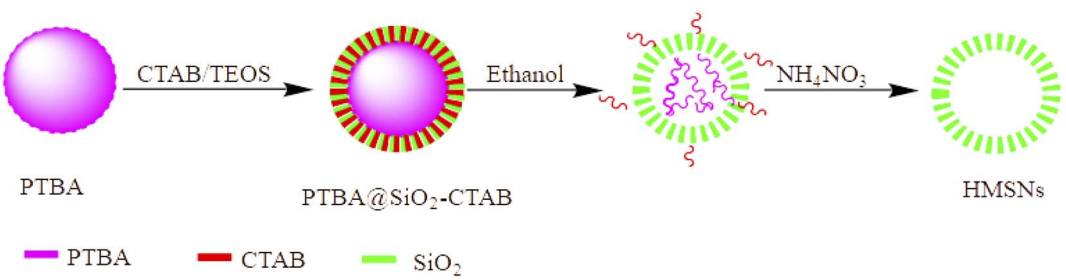

Fig. 3 The process of preparing HMSNs by soft template method.

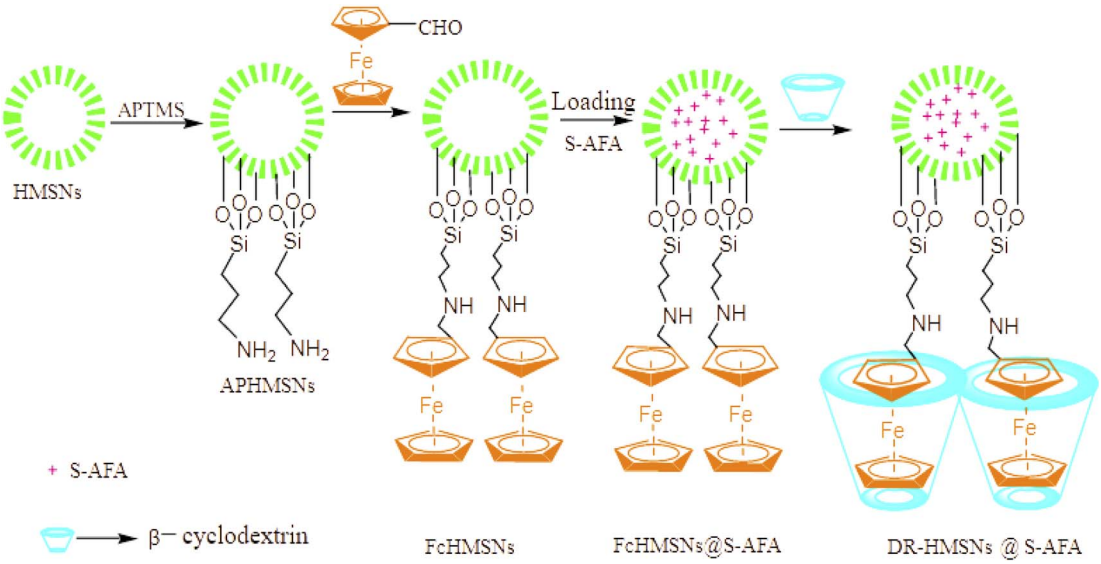

Fig. 4 DR-HMSNs@S-AFA preparation process.

the β-cyclodextrin containing ferrocene nano valves can be used as a switch in response to both REDOX potential and pH. The sustained release performance of dual-response nanoparticles is affected by many factors, including the concentration of oxidant and pH value of medium. In this paper, the fluorescence emission spectra of samples were measured by fluorescence spectrophotometer to verify the response of DR-HMSNs@S-AFA to REDOX and pH.

3. Results and discussion

3.1. SEM and TEM characterization of HMSNs nanoparticles

SEM and TEM images of HMSNs nanoparticles prepared by soft template method are shown in Fig. 5.

As can be seen from SEM and TEM images, the sphericity of HMSNs prepared by this method is good, the spherical shell is intact without damage, and the particle size uniformity and dispersion are also ideal. The wall thickness is very uniform (50 nm), and the particle size is about 250 nm. Meanwhile, the three-dimensional sphere structure of the nanocontainer is obvious, and the nanoparticles have obvious hollow and mesoporous structures.

3.2. BET test of HMSNs nanoparticles

BET specific surface area test and BJH pore size distribution analysis were performed on HMSNs samples, and the results are shown in the Fig. 6.

As can be seen from the Fig. 6, the nitrogen adsorption type of HMSNs obtained by soft template method in this paper is type IV, with obvious hysteresis loops, which further confirms the existence of hollow and mesoporous channels. As can be seen from the BJH pore size distribution diagram, the mesoporous diameter of the nanoparticles is 4.0 nm, the specific surface area is $896 \pm 0.5\ m^2\ g^{-1}$, and the pore volume is $0.83\ cm^3\ g^{-1}$.

3.3. FTIR characterization of functionalized HMSNs nanoparticles

Infrared spectra of HMSNs, APHMSNs, FcHMSNs and DR-HMSNs@S-AFA were characterized by a (VERTEX 70) infrared spectrometer produced by Bruker, Germany. The *IR* spectra are shown as Fig. 7.

HMSNs, namely $SiO_2 \cdot nH_2O$, have characteristic functional groups of Si–O–Si and Si–OH. The strong and wide peak at $1085\ cm^{-1}$ is caused by the stretching vibration of Si–O–Si. The peak at $795\ cm^{-1}$ was caused by the bending vibration of Si–O–Si bond and appeared in the infrared spectra of four samples. The broad and strong peak at $3450\ cm^{-1}$ is caused by the stretching vibration of –OH in Si–OH. The broad and weak peak at $2050\ cm^{-1}$ was caused by template PTBA. The peaks at $2985\ cm^{-1}$ and $2930\ cm^{-1}$ disappeared in the DR-HMSNs@S-AFA spectrum after repeated washing with absolute ethanol, which was mainly caused by the removal of organic matter by washing.

After the modification of APTMS, a large amount of $-NH_2$ was introduced into –NH, and a peak was generated by the stretching vibration of N–H at $3430\ cm^{-1}$, and the peaks at $2940\ cm^{-1}$ and $1605\ cm^{-1}$ were generated by the stretching vibration and bending vibration of C–H. FcHMSNs changed from two weak peaks of APHMSNs to a slightly strong peak at $2935\ cm^{-1}$, which was caused by the C–H stretching vibration on the ferrocene ring. A new peak was generated at $1570\ cm^{-1}$, which was caused by the stretching vibration of C=C in ferrocene, which proved the successful introduction of ferrocene. Compared with FcHMSNs, the –OH peak of DR-HMSNs@S-AFA at $3420\ cm^{-1}$ was significantly enhanced because of the loaded S-AFA and blocked mesoporous β-cyclodextrin introduced a lot of –OH; the peak at $1150\ cm^{-1}$ is due to β-cyclodextrin of the C–O–C bond.

The above infrared spectra proved the successful modification of each step from HMSNs → APHMSNs → FcHMSNs → DR-HMSNs@S-AFA and the successful preparation of dual-response acidizing corrosion inhibitor.

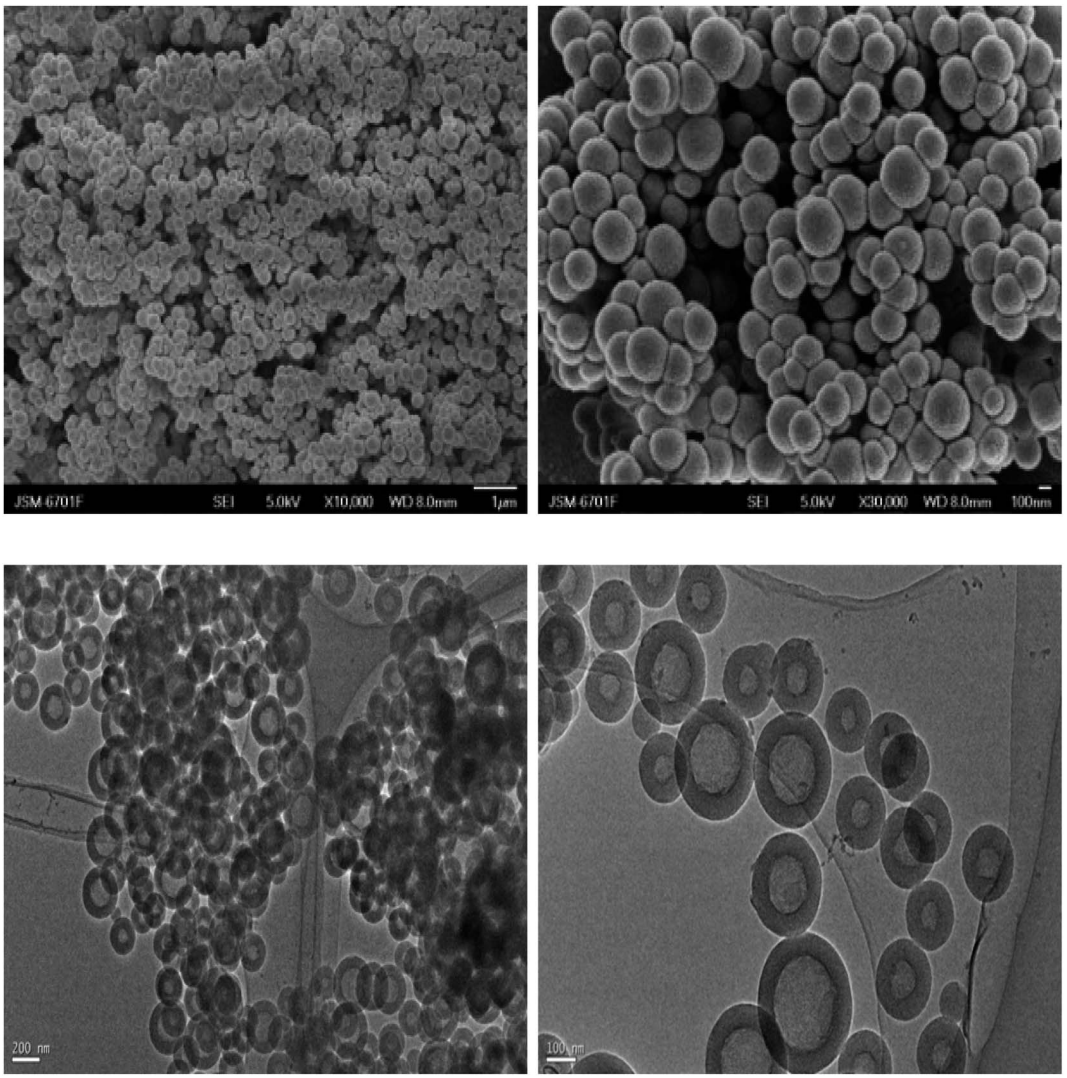

Fig. 5 SEM and TEM images of HMSNs obtained by soft template method.

3.4. SEM characterization of functionalized HMSNs nanoparticles

In this paper, FE-SEM of field emission scanning electron microscope (ZEISS GeminiSEM 500) produced by German Carl ZEISS Company was used to conduct SEM characterization of HMSNs, FcHMSNs and DR-HMSNs@S-AFA. The results are shown in the Fig. 8:

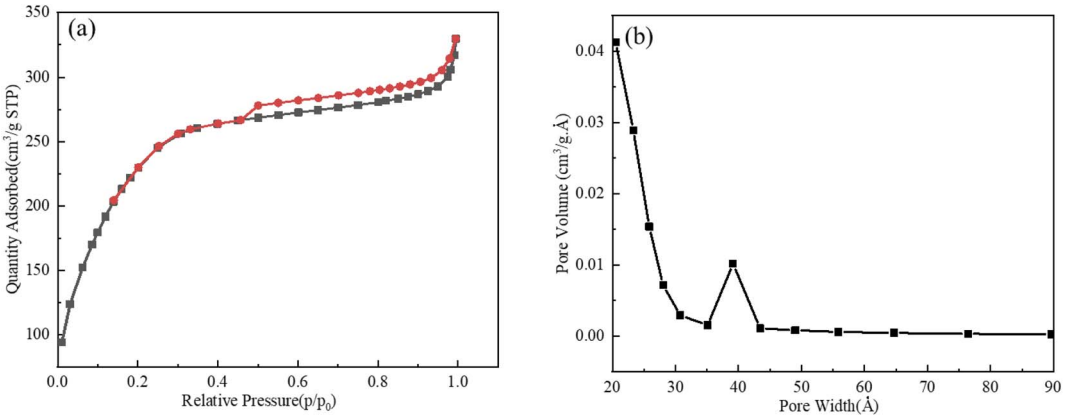

Fig. 6 (a) Nitrogen adsorption–desorption isotherms and (b) pore size distribution of HMSNs obtained by soft template method.

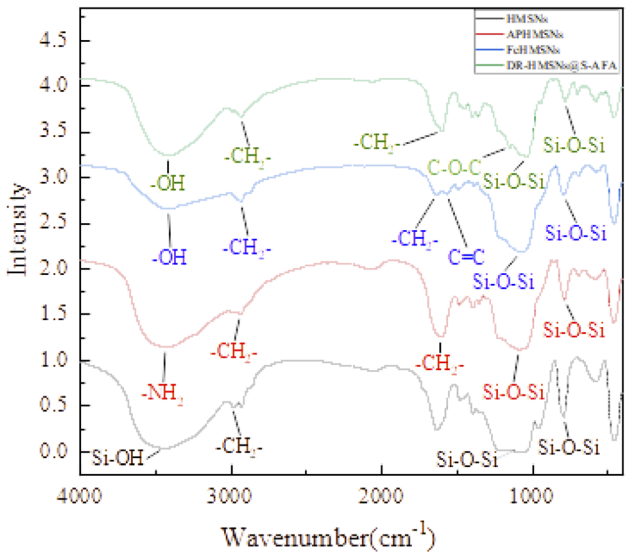

Fig. 7 *IR* spectra of different HMSNs.

As can be seen from the Fig. 8, compared with HMSNs prepared by soft template method, the sphericity, particle size uniformity and dispersion of FcHMSNs obtained by initial modification of amino group and grafting of ferrocene formaldehyde are slightly worse. The reason is that the amino carbon chain and ferrocene group grafted to the mesopore and surface of HMSNs will be twisted due to the length of the chain, thus affecting its structure. Compared with FcHMSNs, the sphericity, particle size uniformity and dispersion of DR-HMSNs@S-AFA obtained by β-cyclodextrin inclusion were improved. The reason is that β-cyclodextrin is a steric hindrance structure, and there is inclusion cooperation between ferrocene group and β-cyclodextrin, resulting in better dispersion of DR-HMSNs@S-AFA.

3.5. EDS analysis

Through EDS element analysis, it can be qualitatively determined whether HMSNs is loaded with acid corrosion inhibitor (S-AFA), and the results are shown in the Fig. 9.

3.6. Controlled release experiment

Iron products mainly undergo oxygen absorption corrosion, so the responsive release function of DR-HMSNs@S-AFA was tested by simulating the corrosion environment of carbon steel. The premature release of S-AFA from DR-HMSNs@S-AFA in ethanol solution with pH = 6 was studied before adding pH and REDOX initiator. 3 mL solution was taken out at 24 h, 36 h, 48 h and 144 h, respectively, and the fluorescence spectra of the solution in the preceding *n* hours were measured. The differences among the five fluorescence spectra measured under different durations were used to obtain the controlled release of DR-HMSNs@S-AFA on acidification corrosion inhibitor in ethanol solution with pH = 6, as shown in Fig. 10. (a) The fluorescence spectra of S-AFA released by DR-HMSNs@S-AFA in ethanol solution with pH = 6 and excitation wavelength of 321 nm; (b) the relationship between the release rate of DR-HMSNs@S-AFA and time.

As can be seen from Fig. 10, in ethanol solution with pH = 6, the premature release of S-AFA within 6 days is basically negligible. It can be seen from Fig. 10(b) that a small amount of drug was released within 6 days, which may be caused by partial loss of

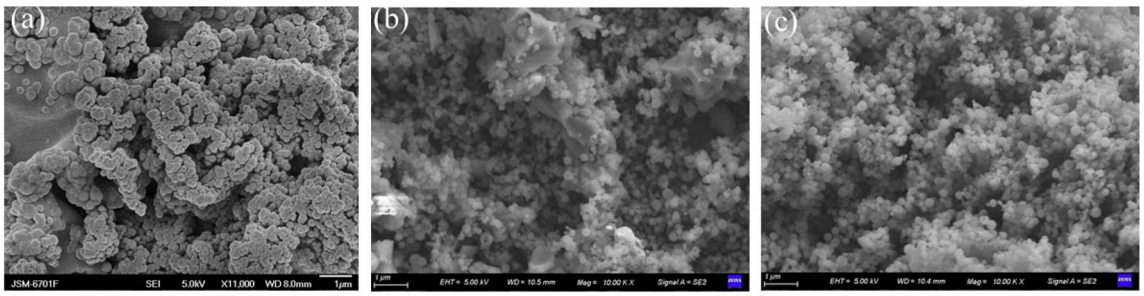

Fig. 8 SEM of (a) HMSNs; (b) FcHMSNs; (c) DR-HMSNs@S-AFA.

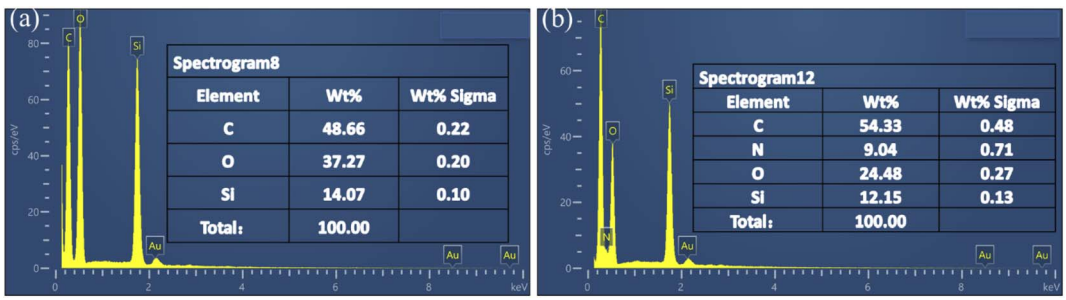

Fig. 9 EDS diagram of (a) HMSNs before and (b) after loading acidizing inhibitor.

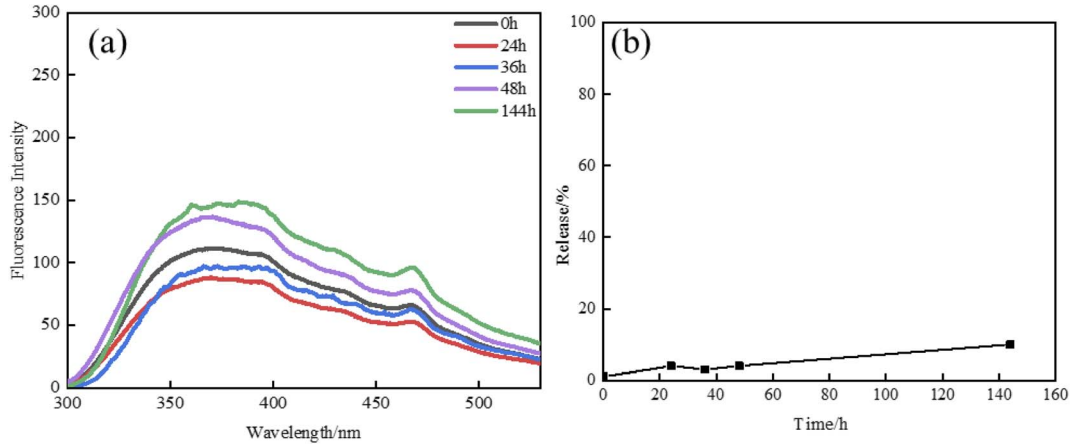

Fig. 10 (a) Fluorescence spectrum of DR-HMSNs@S-AFA acidizing corrosion inhibitor and (b) its release rate changing with time.

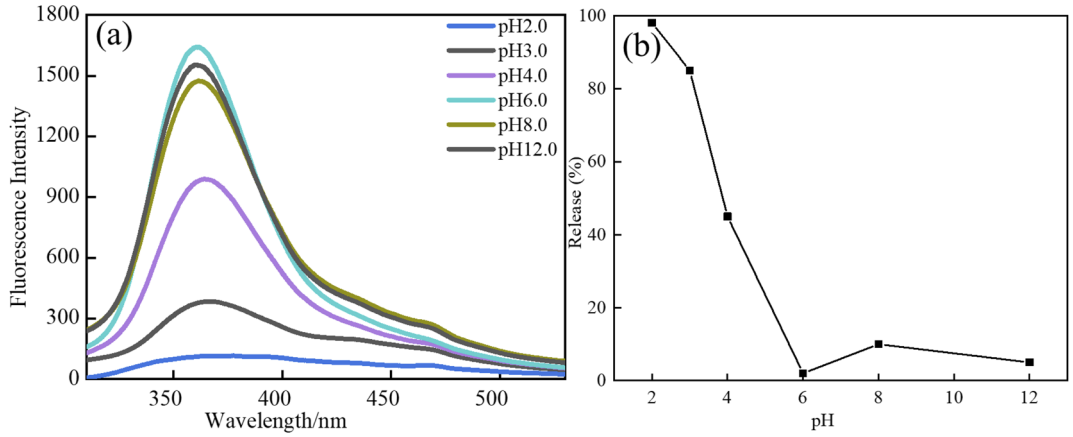

Fig. 11 (a) Fluorescence spectrum and (b) release rate of S-AFA of DR-HMSNs@S-AFA varying with pH.

corrosion inhibitor adsorbed on the surface of DR-HMSNs@S-AFA. The small amount of drug release showed that β-cyclodextrin containing ferrocene nano valves had good sealing property and could prevent the premature release of S-AFA.

3.7. pH

According to 3.6, before the addition of pH trigger agent, the premature release of acidizing corrosion inhibitor in ethanol solution with pH = 6 can be basically ignored. In order to further verify whether DR-HMSNs@S-AFA can realize the response to pH changes, controlled release tests were carried out on the sustained-release dual-response nanoparticles coated with acidizing corrosion inhibitor under different pH environments. The results are shown in Fig. 11(a): fluorescence spectra of S-AFA released by DR-HMSNs@S-AFA in ethanol solutions with different pH and excitation wavelength of 321 nm Fig. 11(b): the relationship between the release rate of DR-HMsn@S-AFA and pH.

Fig. 11 showed that dual-response nanoparticles can achieve rapid release under optimal conditions. Under neutral or alkaline conditions, the release of acidizing corrosion inhibitor is less than 10%, which can be ignored. With increasing acidity, the release of acidizing corrosion inhibitor is more and more. Under strong acidic condition pH = 2.0, the acid inhibitor can be released completely. This is due to the oxidation of Ferrocene group by O_2 in the acid-catalyzed environment. The ferrocene group used for inclusion in β-cyclodextrin was reduced to ferrocene and lost inclusion, resulting in the separation between the host and the guest of the nano valves, resulting in the formation of pores, resulting in the escape of acidizing corrosion inhibitor molecules.

3.8. Concentration of oxidant

In 3.7, the response of DR-HMSNs@S-AFA to pH was studied, and it was found that the acidizing corrosion inhibitor could be basically released completely under strong acidic conditions. In the ethanol solution of DR-HMSNs@S-AFA (pH = 6), oxidizer 30% H_2O_2 of different concentrations was added to conduct response release tests under different REDOX environments. The results are shown in Fig. 12. (a) Fluorescence spectra of S-AFA released by DR-HMSNs@S-AFA in ethanol solutions with different oxidant concentrations and excitation wavelength of 321 nm. (b) The relationship between the release rate of DR-HMSNs@S-AFA and oxidant concentration.

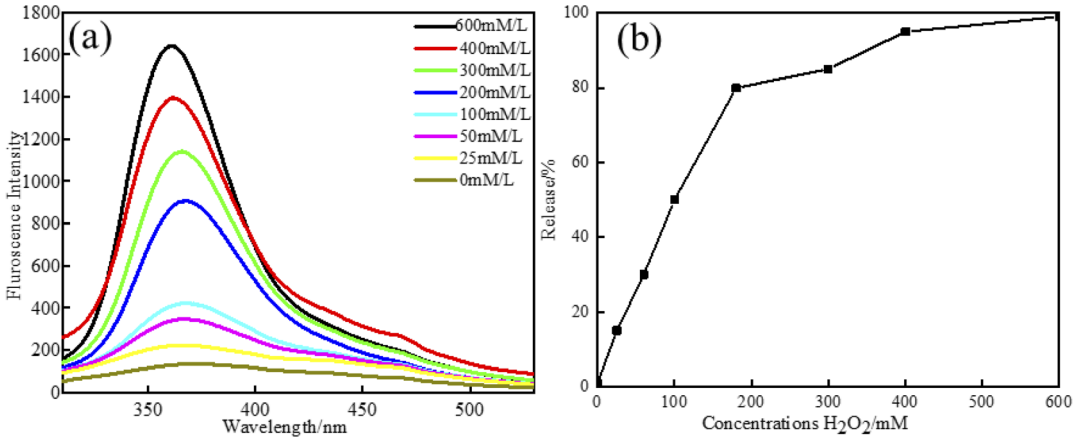

Fig. 12 (a) Release of DR-HMSNs@S-AFA fluorescence spectrum of S-AFA and (b) the change of release rate with the concentration of oxidizer.

It can be seen from Fig. 12 that DR-HMSNs@S-AFA nano valves control system can basically achieve "zero release" when H_2O_2 is not added into the system, and "100%" release of S-AFA can be achieved when H_2O_2 is added about 600 mM. The reason is that H_2O_2 partially oxidizes ferrocene to ferrocene monomer and induces the rapid release of acidizing corrosion inhibitor.

4. Conclusion

In this paper, a kind of HMSNs nanocontainers loaded with acidification inhibitor was prepared by soft template method. A β-cyclodextrin coated ferrocene nano valves was designed and assembled, and its release in response to REDOX and pH was explored. Using very uniform and stable white PTBA emulsion droplets as template, the hollow and mesopic structure of HMSNs was ideal. The vessel was modified by amino group and then grafted with ferrocene group to obtain an interesting vessel, which was loaded with acidifying inhibitor through impregnation method and negative pressure method, and finally was successfully prepared by β-cyclodextrin encapsulation dual response acidifying corrosion inhibitor. Rapid response release can be achieved when pH = 2 or H_2O_2 concentration is 600 mL^{-1}, and basically no release is achieved under alkaline or neutral conditions or when H_2O_2 concentration is too small. The results show that the microenvironment-sensitive carrier has excellent performance and has application value in the on-demand release of active substances.

Conflicts of interest

There are no conflicts to declare.

References

1 Z. Yang, Z. Wang and W. E. I. Peng, Application of stimulus-responsive liposomes in targeted drug delivery systems, *Chin. J. Biochem. Mol. Biol.*, 2020, **36**(12), 1395–1403.
2 W. H. Xu, N. Li, D. Zeng, *et al.*, Research progress of metal-organic framework in drug delivery stimulus response system, *J. Huazhong Univ. Sci. Technol. Med. Sci. J.*, 2022, **36**(1), 4.
3 X. Y. Tyrum, H. B. Yuan, J. Gao, *et al.*, Application of stimulus-responsive hydrogels in controlled drug release, *J. Hebei Univ. Technol.*, 2021, **50**(5), 8.
4 Y. Fan, H. A. O. Wenyan, S. Zhang, *et al.*, Research Progress on New Mechanisms of "Intelligent" Drug Carrier Modulation, *Chin. J. New Drugs*, 2021, **30**(21), 8.
5 Y. Guo, H. Liu, S. Li, *et al.*, Research Progress on Stimulation Response and Delivery of Antitumor Drugs by Targeted Mesoporous Silica Nanoparticles, *Chem. Eng. Sci.*, 2021, **38**(8), 8.
6 X. U. Yong-quan, L. I. Kai, R.-H. Zhao, *et al.*, *Method for Preparing Hollow Mesoporous Silica Nanosphere Supported Propranolol Hydrochloride Composite System*, CN112678836A, 2021.
7 Q. Zhong, S. Zhou, X. Wang, *et al.*, Construction of Mesoporous Silica-based Intelligent Delivery System and Its Application in the Treatment of Various Diseases, *Chem*, 2022, **34**(3), 696–716.
8 X. Wang, Z. Gong, M. Yan, *et al.*, Preparation and Evaluation of pH-responsive Hollow Mesoporous Silica Nanoparticles Modified by RGD Peptide, *Chem. Eng. Sci.*, 2021, **38**(9), 7.
9 L. I. Yan, Y. Duan, M. Wei, *et al.*, *Preparation method and application of an intelligent controlled-release targeted nano-flooding agent microcapsule*, CN112538145A, 2021.
10 G. Liu, Zhejiang University successfully established a system for the efficient control of acid-controlled Ber@ZnO-ZIF-8 nano pesticide preparations for the efficient control of fanqian green blight, *Pesticide Market Information*, 2022 (7) p. 1.
11 W. Xu, Z. Yang, G. Y. Zhang, *et al.*, Photo-Temperature Dual Response Pesticide Release System for Mesoporous Silica Nanoparticles Based on Dopamine Modification, *J. Cent. South Univ.*, 2022, **29**(2), 13.
12 M. Chen, X. Jin, X. Ma, *et al.*, Click Preparation and Application of Chiral Chromatography Media Based on Cyclodextrin Eigen Recognition Ability, *Chromatography*, 2020, **38**(11), 1270–1280.

13 C. Y. Duan, J. Kong, H. E. Cheng, *et al.*, *Reactive NMR contrast agent based on nacridamide as the identification site and its preparation method*, CN103463647B, 2015.
14 J. Zhao, Q. Su, Y. Wang, *et al.*, Research Progress on Self-Healing of Polymer Materials by β-Cyclodextrin Subject and Guest Molecules, *Chem. Fiber Text. Technol.*, 2021, **50**(4), 2.
15 H. U. A. N. G. Liang, H. Xu, W. Xiong, *et al.*, Homogeneous Electrochemical Aptamer Sensor for Sensitive Detection of Thrombin Based on Amplification of Host-Object Recognition Pattern Signal between Bis-Ferrocene and β-Cyclodextrin, *Laboratory of Analytical Analysis*, 2021, **40**(4), 5.
16 J. X. Li, T. Kuang Chun, L. H. Zhang, *et al.*, Effects of temperature and pH on the supramolecular effects of curcumin and hydroxypropyl-β-cyclodextrin, *World J. Chem.*, 2021, **62**(11), 5.
17 A. L. ParraGuardado, C. L. Sweeney, E. K. Hayes, *et al.*, *Development of a rapid pre-concentration protocol and a magnetic beads-based RNA extraction method for SARS-CoV-2 detection in raw municipal wastewater*, 2021.
18 Z. Chen, P. Li, X. Zhang, *et al.*, Reticular exploration of uranium-based metal-organic frameworks with hexacarboxylate building units, *Nano Res.*, 2021, **14**, 376–380.
19 I. Roy and J. F. Stoddart, Cyclodextrin Metal-Organic Frameworks and Their Applications, *Acc. Chem. Res.*, 2021, **54**(6), 1440–1453.
20 Y. He, L. Chen, R. He, *et al.*, Research Progress on Construction of Fluorescent Probes by Cyclodextrin Derivatives and Clathrates, *Chin. J. Org. Chem.*, 2022, **42**(3), 785–795.